

High Time-Resolved Three-Dimensional Imaging Using Ultrafast Optical Kerr Gate of Bismuth Glass

Wenjiang Tan, Junyi Tong, Jinhai Si, Yi Yang, Wenhui Yi, Feng Chen, and Xun Hou

Abstract—We have demonstrated the high time-resolved three-dimensional (3-D) imaging using a chirped supercontinuum (SC) and an ultrafast optical Kerr gate (OKG) generated with a femtosecond laser, in which a sapphire plate and a $\text{Bi}_2\text{O}_3\text{-B}_2\text{O}_3\text{-SiO}_2$ oxide glass (BI glass) were used to generate the chirped SC and the optical Kerr gate, respectively. The experimental results show that the 3-D imaging using BI glass offers better temporal and longitudinal spatial resolution compared with CS_2 .

Index Terms—Bismuth compounds, nonlinear optics, optical Kerr effect.

I. INTRODUCTION

TIME-RESOLVED imaging based on optical Kerr gate (OKG) has provided an interesting tool for scientific research and various potential applications. This imaging technique was first proposed by Alfano *et al.*, and used to the ballistic optical imaging for objects hidden in scattering media, such as high-pressure diesel sprays and liquid jets in gaseous crossflow [1]–[4]. Combining with a chirped supercontinuum (SC), OKG was also used to realize the simultaneous three dimensional (3-D) imaging [5]–[7]. Moreover, time-resolved imaging based on OKG was an effective method to diagnose various ultrafast phenomena, such as ultrafast fluorescence, laser-produced plasmas and propagation dynamics of laser pulses in a medium [8]–[12].

However, there is an inherent trade-off between high sensitivity and fast response in the applications based on OKG in femtosecond regime. For example, Carbon disulfide (CS_2) is widely used as the Kerr medium due to its large optical nonlinearity. However, it suffers a slow relaxation time as long as 1.6 ps [13]. Recently, it has emerged that heavy metal oxide glasses seem to be preferable candidates as the Kerr media due to their large optical nonlinearities, ultrafast response time, and wide transparent window, which could offer better temporal resolution, higher signal-to-noise ratio, and wider applicable wavelength range [14]–[18].

Manuscript received October 23, 2010; revised January 15, 2011; accepted January 22, 2011. Date of publication January 31, 2011; date of current version March 23, 2011. This work was supported by the National Science Foundation of China under Grant 11074197 and Grant 60978015, by the National High Technology R&D Program of China under Grant 2009AA04Z305, and by the Specialized Research Fund for the Doctoral Program of Higher Education of China (Grant 200806980022).

The authors are with the Key Laboratory for Physical Electronics and Devices, Ministry of Education, and Shaanxi Key Laboratory of Information Photonic Technique, School of Electronics and Information Engineering, Xi'an Jiaotong University, Xi'an 710049, China (e-mail: jinhaisi@mail.xjtu.edu.cn).

Color versions of one or more of the figures in this letter are available online at <http://ieeexplore.ieee.org>.

Digital Object Identifier 10.1109/LPT.2011.2109704

II. EXPERIMENTS AND METHODS

In this study, a nonresonant-type $\text{Bi}_2\text{O}_3\text{-B}_2\text{O}_3\text{-SiO}_2$ oxide glass (BI glass) containing 70% Bi_2O_3 was used as the Kerr medium to demonstrate the time-resolved 3-D imaging. One two-dimensional (2-D) true color image was obtained using the ultrafast OKG and a chirped SC. The Kerr-gated spectra corresponding to the 2-D image were also measured at two different time delays, demonstrating that the 3-D imaging using BI glass offers better temporal and longitudinal spatial resolution comparing with CS_2 .

The BI glass sample was prepared by the melting method, the composition of which was 70%- $\text{BiO}_{1.5}$, 10%- SiO_2 , 10%- B_2O_3 , and 0.15%- GeO_2 (mol%). The details about the preparation of the sample were shown elsewhere [14]. The nonlinear response time of the BI glass has been measured to be less than 85 fs, the origin of nonlinearities of which arises from electronic polarization [17]. The nonlinear refractive-index n_2 of the BI glass is measured to be $1.6 \times 10^{-14} \text{ cm}^2/\text{W}$, which is comparable to that of chalcogenide glasses [18].

A Ti:sapphire laser system with a repetition rate of 1 kHz, pulse duration of 30 fs and an average power of 1 W at 800 nm, was used in our experiments. The emitting fundamental laser beam was split into two beams by means of a 20/80 beam splitter. Passing through an optical delay translation stage, the intense one was finally focused onto the Kerr medium as the gating beam. In order to get higher signal-to-noise ratio and better time resolution, a 1-mm BI glass sample was chosen as the Kerr medium. The CS_2 solution was also filled in a 1-mm quartz cuvette. A half-wave plate was used to rotate the polarization of the gating beam by $\pi/4$. The weak beam was focused into a 3-mm sapphire plate to obtain a stable SC as the probe beam. The probe beam was collimated and expanded to illuminate a transparent object which was a piece of glass sheet composed of four flat steps as shown in Fig. 1. The OKG consisted of a pair of crossed polarizers and the Kerr medium between them. When the OKG was opened by the gating beam, a time-sliced probe beam passed through the analyzer and was synchronously detected with a color charged-coupled device (CCD) camera and a micro spectrometer. To block light at the fundamental 800 nm wavelength, two cutoff filters were placed before the CCD and the micro spectrometer, respectively.

Fig. 1 shows the schematic of the 3-D imaging. In our experiments, the thicknesses for the regions I, II, III, IV of the object were 150, 300, 1080, and 1230 μm , respectively. After passing through the object, the probe beam had different optical paths for the regions I, II, III, IV. By adjusting the time delay between the gating pulse and the SC, the OKG could transmit

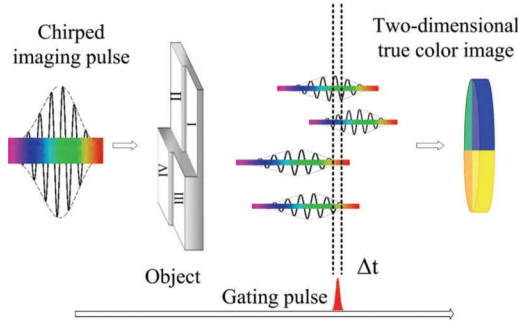


Fig. 1. Schematic of the high time-resolved 3-D imaging technique using chirped SC and OKG.

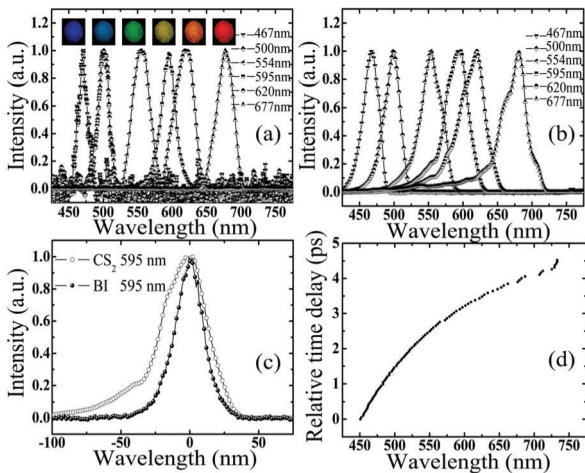


Fig. 2. Kerr-gated spectra from the SC. (a) Kerr-gated spectra from the SC at six selected wavelengths obtained using the BI glass. The inset shows the corresponding beam patterns of the Kerr-gated spectra; (b) Kerr-gated spectra from the SC at the same six selected wavelengths obtained using CS_2 ; (c) comparison of the Kerr-gated spectra at the peak wavelength of 595 nm; (d) chirp structure of the SC.

a time-sliced SC with four wavelengths, which was detected by a color CCD. The spectral information was also monitored by a micro spectrometer synchronously. The transmitted beam showed a color distribution according to the surface structure, so we could obtain a real-time colored 3-D map of the object.

III. RESULTS AND DISCUSSION

We firstly studied the characteristics of Kerr-gated spectra acquired from the chirp SC using the BI glass and CS_2 , respectively, in which the object was removed. A series of Kerr-gated spectra at six different wavelengths are shown in Fig. 2(a) and (b). The corresponding beam patterns obtained using the BI glass are also shown in the inset of Fig. 2(a). From Fig. 2(a) and (b), we can see that the Kerr-gated spectra obtained using the BI glass have narrower bandwidth and more symmetrical distribution. A typical Kerr-gated spectrum with the peak wavelength at 595 nm, as shown in Fig. 2(c), was chosen to illustrate further the difference between Kerr-gated spectra obtained using the BI glass and that using CS_2 . The bandwidth of Kerr-gated spectrum obtained using the BI glass is about 25 nm in full width at half maximum (FWHM). The Kerr-gated spectrum obtained using CS_2 exhibits an obvious

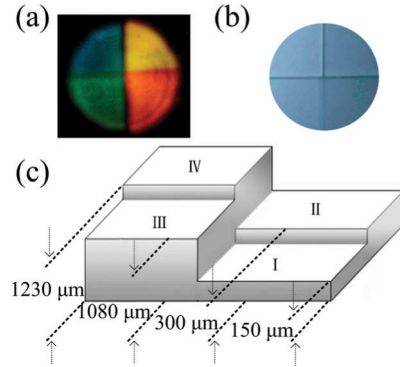


Fig. 3. Images of the object. (a) Kerr-gated true 2-D color image of the circular illuminated area of the object obtained using the BI glass; (b) photograph of the object obtained using a CCD camera; (c) schematic diagram of the object.

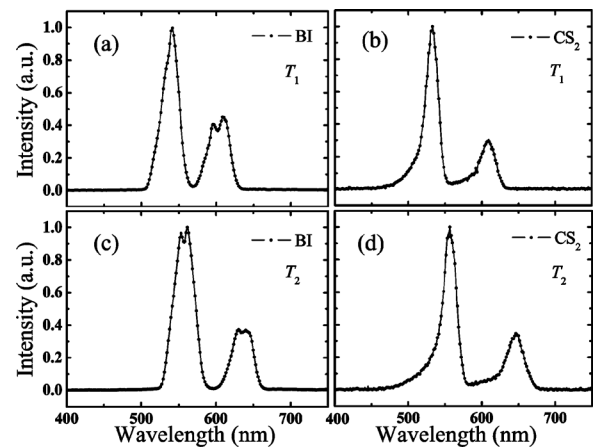


Fig. 4. Kerr-gated spectra of the imaging object at two time delays. (a) Using BI glass as the Kerr medium at the time delay T_1 ; (b) using CS_2 as the Kerr medium at the time delay T_1 ; (c) using BI glass as the Kerr medium at the time delay T_2 ; (d) using CS_2 as the Kerr medium at the time delay T_2 .

band tailing. This is because the nonlinear response of the BI glass is much faster than that of CS_2 . Therefore the BI glass could offer better temporal and longitudinal spatial resolution. Fig. 2(d) presents the relative time delays versus the various peak wavelengths of the overall Kerr-gated spectra. The SC expands nonlinearly to 4.6 ps in time domain, the spectrum of which ranges from 450 nm to 750 nm. This chirp characteristic of the SC originates mainly from the nonlinear dispersion effect in the sapphire [19].

Furthermore, we demonstrated the 3-D imaging using the chirped SC and the BI glass. The Kerr-gated image of the object is shown in Fig. 3(a), while the photograph and schematic of the object are shown in Fig. 3(b) and (c), respectively. There are four colored regions, i.e., cyan, green, yellow, and orange, in Fig. 3(a), corresponding to regions I, II, III, and IV of the object, respectively.

In addition, we also measured the Kerr-gated spectra of the images as shown in Fig. 3(a) at different time delays, which are shown in Fig. 4. From Fig. 4(a), we can see that when the BI glass is used and the delay time is set at T_1 , there are only three distinguishable peaks in the Kerr-gated spectrum. The two peaks in the longer-wavelength region correspond to the region III and IV of the object, respectively, while the peak of the

shorter-wavelength corresponds to the combination of the region I and II of the object. The reason is that the SC has a more slowly frequency-chirped characteristic for the shorter-wavelength components than that for the longer-wavelength components as shown in Fig. 2(d). By adjusting the time delay, we got another Kerr-gated spectrum of the object at the time delay T_2 , which has four peaks as shown in Fig. 4(c). In our experiments, the opening time of the OKG for the BI glass was expanded to about 250 fs due to the dispersion of the optical elements. In case of CS_2 , there are only two peaks of the Kerr-gated spectra at the both time delays as shown in Fig. 4(b) and (d), because the nonlinear response of CS_2 is much slower than that of the BI glass. These results further demonstrate that the 3-D imaging using the BI glass has better temporal and longitudinal spatial resolution compared with CS_2 .

It should be mentioned that for a reflection-type 3-D imaging, a higher longitudinal resolution could be obtained. The explanation is described as follows: The longitudinal resolution is dependent on the optical path difference corresponding to the different regions on the object surface. For the reflection-type imaging, the optical path difference is twice the step height on the object surface, while for the transmission-type imaging, the optical path difference is equal to the product of the step height and the refractive index difference between air and the object.

IV. CONCLUSION

In conclusion, we have demonstrated the high time-resolved 3-D imaging using the ultrafast OKG of the BI glass and the chirped SC. The Kerr-gated spectra obtained using BI glass and CS_2 were also measured at two different time delays, demonstrating that the 3-D imaging obtained using BI glass offers better temporal and longitudinal spatial resolution compared with CS_2 .

REFERENCES

[1] L. Wang, P. P. Ho, C. Liu, G. Zhang, and R. R. Alfano, "Ballistic 2-D imaging through scattering walls using an ultrafast optical Kerr gate," *Science*, vol. 253, pp. 769–771, 1991.
 [2] R. R. Alfano, X. Liang, L. Wang, and P. P. Ho, "Time-Resolved imaging of translucent droplets in highly scattering turbid media," *Science*, vol. 264, pp. 1913–1915, 1994.

[3] M. A. Linne, M. Paciaroni, J. R. Gord, and T. R. Meyer, "Ballistic imaging of the liquid core for a steady jet in crossflow," *Appl. Opt.*, vol. 44, pp. 6627–6634, 2005.
 [4] J. B. Schmidt, Z. D. Schaefer, T. R. Meyer, S. Roy, S. A. Danczyk, and J. R. Gord, "Ultrafast time-gated ballistic-photon imaging and shadowgraphy in optically dense rocket sprays," *Appl. Opt.*, vol. 48, pp. B137–B144, 2009.
 [5] R. Dorsinville, P. P. Ho, J. T. Manassah, and R. R. Alfano, *The Supercontinuum Laser Source: Fundamentals With Updated References*, R. R. Alfano, Ed. New York: Springer, 2006, ch. 9.
 [6] K. Minoshima, T. Yagi, E. Abraham, and H. Matsumoto, "Three-dimensional imaging using a femtosecond amplifying optical Kerr gate," *Opt. Eng.*, vol. 38, pp. 1758–1762, 1999.
 [7] T. Yasui, K. Minoshima, and H. Matsumoto, "Three-dimensional shape measurement of a diffusing surface by use of a femtosecond amplifying optical Kerr gate," *Appl. Opt.*, vol. 39, pp. 65–71, 2000.
 [8] T. Fujino, T. Fujima, and T. Taharab, "Picosecond time-resolved imaging by nonscanning fluorescence Kerr gate microscope," *Appl. Phys. Lett.*, vol. 87, pp. 131105-1–131105-3, 2005.
 [9] L. Gundlach and P. Piotrowiak, "Femtosecond Kerr-gated wide-field fluorescence microscopy," *Opt. Lett.*, vol. 33, pp. 992–994, 2003.
 [10] D. R. Symes, U. Wegner, H.-C. Ahlswede, M. J. V. Streeter, P. L. Gallegos, E. J. Divall, R. A. Smith, P. P. Rajeev, and D. Neely, "Ultrafast gated imaging of laser produced plasmas using the optical Kerr effect," *Appl. Phys. Lett.*, vol. 96, pp. 011109-1–011109-3, 2010.
 [11] M. Fujimoto, S. Aoshima, and Y. Tsuchiya, "Multiframe observation of an intense femtosecond optical pulse propagating in air," *Opt. Lett.*, vol. 27, pp. 309–311, 2002.
 [12] R. Nakamura and Y. Kanematsu, "Femtosecond spectral snapshots based on electronic optical Kerr effect," *Rev. Sci. Instrum.*, vol. 75, pp. 636–644, 1996.
 [13] R. A. Ganeev, A. I. Rysanyansky, M. Baba, M. Suzuki, N. Ishizawa, M. Turu, S. Sakakibara, and H. Kuroda, "Nonlinear refraction in CS_2 ," *Appl. Phys. B*, vol. 78, pp. 433–438, 2004.
 [14] N. Sugimoto, H. Kanbara, S. Fujiwara, K. Tanaka, and Y. Shimizu-gawa, "Third-order optical nonlinearities and their ultrafast response in $\text{Bi}_2\text{O}_3 - \text{B}_2\text{O}_3 - \text{SiO}_2$ glasses," *J. Opt. Soc. Amer. B*, vol. 11, pp. 1904–1908, 1999.
 [15] B. L. Yu, A. B. Bykov, T. Qiu, P. P. Ho, R. R. Alfano, and N. Borrelli, "Femtosecond optical Kerr shutter using lead-bismuth-gallium oxide glass," *Opt. Commun.*, vol. 215, pp. 407–411, 2003.
 [16] S. Zhou, H. Dong, H. Zeng, G. Feng, H. Yang, B. Zhu, and J. Qiu, "Broadband optical amplification in Bi-doped germanium silicate glass," *Appl. Phys. Lett.*, vol. 91, pp. 061919-1–061919-3, 2007.
 [17] W. Tan, H. Liu, J. Si, and X. Hou, "Control of the gated spectra with narrow bandwidth from a supercontinuum using ultrafast optical Kerr gate of bismuth glass," *Appl. Phys. Lett.*, vol. 93, pp. 051109-1–051109-3, 2008.
 [18] T. Lin, Q. Yang, J. Si, T. Chen, X. Wang, X. Hou, and K. Hirao, "Ultrafast nonlinear optical properties of $\text{Bi}_2\text{O}_3 - \text{B}_2\text{O}_3 - \text{SiO}_2$ oxide glass," *Opt. Commun.*, vol. 275, pp. 230–233, 2007.
 [19] C. Nagura, A. Suda, H. Kawano, M. Obara, and K. Midorikawa, "Generation and characterization of ultrafast white-light continuum in condensed media," *Appl. Opt.*, vol. 41, pp. 3735–3742, 2002.